IOP Conference Series: Materials Science and Engineering

Molecular Dynamics Simulation of the Tensile Properties of an Al6063-SiO_2 Composite under Varying Temperature Conditions

Molecular Dynamics Simulation of the Tensile Properties of an Al6063 – SiO_2 Composite under Varying Temperature Conditions

N Idusuyi, A H Adekoya and T T Olugasa

Mechanical Engineering Department, University of Ibadan, Ibadan, Nigeria
nosaidus@gmail.com

Abstract. The tensile stress behaviour of Aluminium Metal Matrix Composites (AMCs) reinforced with SiO_2 was evaluated using Molecular Dynamics (MD). A cubic model was used for the simulation, while the Modified Embedded Atom Method (MEAM) was implemented to describe the atomic interactions for the MD simulation. From the MD simulation the presence of the SiO_2 was found to substantially disrupt the FCC crystallography of the Al and reduce the ductility of the Al while substantially increasing the yield strength of the composite. A Maximum Elastic modulus of 43.3GPa was obtained at a temperature of 350K and 10wt% SiO_2.

1. Introduction

The development of Aluminium Metal Matrix Composites (AMCs) is one of the most significant achievements in the history of materials research and processing [1]. AMCs which exhibit high strength, high elastic modulus and good wear resistance have been developed to meet the requirements of materials for aerospace and automobile applications [2,3]. However, the high costs associated with producing AMCs limits its applications [4,5]. The properties of AMCs are influenced by type of reinforcement (Synthetic ceramic particles, Industrial wastes and agro-wastes) as well as other properties like shape (particulate, volume fraction, bonding type and size [6,7]. Silicon Oxide (SiO_2) is the dominant compound in Rice Husk Ash and other agricultural waste products which have found usefulness as a less expensive reinforcement alternative for the production of MMCs [8–11]. In order to rationalize the experimental observations, researchers have resorted to a theoretical analysis of MMCs by way of atomic simulation[12]. In a study of Al/SiC interfaces by Li et.al [13], it was reported that the bond strength between Al and Al were generally lower than SiC and Al, with the later been up to 1.5 times stronger. Jena [14] however, used a self-consistent quantum mechanical method to determine the binding energies and bond lengths of Al–Al, Al-Si, Al–C and Si–C dimers. Their study discovered that the bonding of Al–C dimers was stronger than others studied, thereby leading to the formation of Al_4C_3 at the interface. Similar observations were made by Lu et al.[15] based on an extended Hückel theory, that the Al–C interaction was stronger and the Al–SiC interaction was confined to a narrow region at the interface. Molecular Dynamics is a powerful technique that utilizes Newton's laws to model the interatomic interactions between the particles on a Nano scale [16]. MD simulations are based on interatomic potentials which can be used to study systems involving millions of atoms and to provide macroscopically predictive results. Some of the more popular MD softwares are Large Scale Atomic/Molecular Massively Parallel Simulator (LAMMPS), Tinker, Materials Studio and Chemistry at Harvard Macromolecular Mechanics (CHARMM), etc.[12,17,18]. At present, there are numerous models of these interatomic potentials. These potentials are generally divided into two

broad categories: (1) Pair Potentials, the most common example of which is the Lennard-Jones Potential, and (2) Many body potentials which include Tersoff, Embedded Atomic Potential (EAM) and Modified Embedded Atomic Potential (MEAM). The potentials are developed individually to describe the interactions between specific elements/atoms [19–24]. However, the true interatomic interactions as described by the Schrödinger equation or Dirac equation for all electrons and nuclei. Ward et.al [25] used MD simulation to study the mechanisms of deformation and failure in Al-Si Nano composites. It was reported that a clear difference in the fracture mechanisms was observed in the Al-Si composites as compared to single-phase Al. It was deduced that the Al/Si interfaces controlled the mechanical behaviour in the Nano composites, reducing the role of bulk metal deformation modes [25]. Other researchers have corroborated the importance of the Matrix/reinforcement interface to the properties of the composite[26–29]. Sedigh et.al [30] used MD simulation to study the influence of nanofiller geometry, temperature and defects on the mechanical properties of Aluminium reinforced with Boron-Nitride Nano sheets and nanotubes respectively. It was concluded that Boron-Nitride Nano sheets was a better reinforcement with higher fracture toughness. From the study, the authors concluded that Boron Nitride/Al Nano composites could be useful in producing lightweight materials critical to the aerospace and automobile industry. In another study, the mechanical properties of light nonporous Carbon nanotubes (CNT)-Aluminium (Al) composites were investigated using atomistic tensile simulations. The reinforcements (CNT) were embedded in Al matrix composites to reduce the weight of Al by 23%, thus large volume fractions of large size CNT were used. Pure aluminium structure was simulated using a FCC lattice structure with 4.046 Å as the lattice constant. A pore with a diameter of 2.58nm was drilled at the centre of the pure aluminium to prepare nonporous Al. The nonporous CNT-Al was prepared by inserting CNT into pure aluminium. The aluminium atoms which were inside the CNT radius were removed by considering van der Waals radius carbon atoms and aluminium atoms. The final core hole sizes of the NP Al and NP CNT-Al were configured with a diameter of 2.58 nm. LAMMPS was the software of choice for the simulations, while Open Visualisation Tool (OVITO) was used for visualising and analysing the LAMMPS output. It was observed that the lightweight nanoporous CNT-Al composite had 105.8, 246.9 and 243.7% improvements in tensile strength, fracture toughness, and elastic modulus, respectively [31]. Literature is sparse on the analysis of SiO_2 reinforced AMCs using Molecular dynamics. In this work, the effects of temperature on the tensile stress behaviour of Aluminium Metal Matrix Composites reinforced with SiO_2 were studied using Molecular Dynamics (MD).

2.0 MD Simulation Steps

2.1 Molecular dynamics simulation

The MEAM potentials used in this study for Al and O were obtained from Angelo and Baskes [22], while the Al–O interaction was obtained from Baskes [23]. The elastic constants calculated by the MEAM potential for Al were C11 =111.09 GPa and C12 = 61.68 GPa. Which correspond almost exactly with the values reported by Dandekar et.al [32].

2.2 The model for the study

The structure of pure aluminium used in this study was a Face Centred Cubic (FCC) structure with a lattice parameter of 4.05Å [33]. SiO_2 has a Diamond structure with a lattice constant of 5.43Â.The model was taken as a cuboid of aluminium atoms with spherical inclusions of silica placed at the centre of the cube as depicted in Figure 1(a –c). The dimensions of the simulation box were fixed at 50Â by 100Â by 50Â, while the spherical infusions of silica had a diameter of 5.4Â. The molecular model containing 15,625 atoms was set up using LAMMPS (Large Scale Atomic/Molecular Massively Parallel Simulator). The interaction between the particles were modelled using MEAM potentials for the Al-Si particles, as well as Tersoff potentials for the SiO_2 particles. The Hybrid method was utilized for the pair style command in LAMMPS to combine the effects of the two potential methods, thus providing a comprehensive model. Subsequently, after setting up the system, the atoms were relaxed to find global minimum energy of the system by doing a systematic conformational search via the Polak-Ribiere version of the conjugate gradient (CG) algorithm. At each

iteration the force gradient is combined with the previous iteration information and used to compute a new search direction which is perpendicular (conjugate) to the previous search direction. The atoms were assigned velocities following a Maxwell-Boltzmann distribution around the desired temperature. An MD simulation was performed on the model at a time step of 0.001 ps (Picosecond), under the isothermal canonical ensemble NVT (constant volume - constant temperature) using a Nosė-Hoover thermostat to control the temperature and keep it constant at 300K. The simulations were performed for models with 0wt%, 2.5wt%, 5wt%, 7.5wt% and 10wt% reinforcements respectively. The Open Visualization Tool (OVITO) was used to visualise the outputs of the simulations. The Elastic modulus of the tensile plots was determined by differentiating a second-degree polynomial equation which was fitted to the Stress-Strain graph.

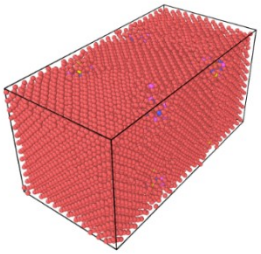

(a)

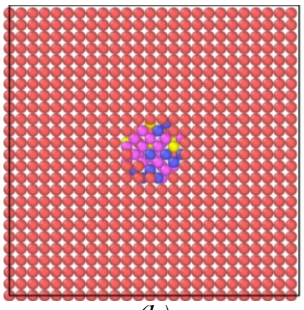

(b)

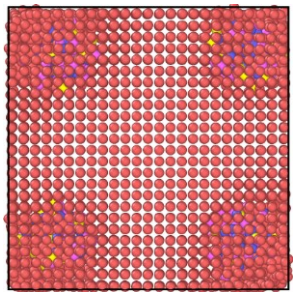

(c).

Figure 1 (a-c) : Aluminium Model for MD Simulation – (a) Cubic Model, (b) Single Unit Cell of model, (c) Agglomeration of Al in Composite Model

Table 1 shows the assumed reinforcement volumes used for the study.

Table 1: Volume Fraction of Composites

Composite	wt.% Al6063	Al6063 (Vol. fraction)	wt.% SiO_2	SiO_2 (Vol. fraction)
Al	100.0	1.0000	0.0	0.0000
Al-2.5wt%SiO_2	97.5	0.9657	2.5	0.0325
Al-5wt% SiO_2	95.0	0.9350	5.0	0.0650
Al-7.5wt% SiO_2	92.5	0.9025	7.5	0.0975
Al-10wt% SiO_2	90.0	0.8700	10.0	0.1300

2.3 Tensile test

The models were stretched at a constant engineering strain of 0.01/femto second under the NVT ensemble. A very low strain rate is desired to ensure the stability of the system. With higher stain rates

(for instance 0.02/femto second), it was observed that the system was unstable under the chosen conditions resulting in either rapid fluctuations in the temperature of the system as the atoms are not given sufficient time to equilibrate before the next step of the iteration. In the other case, the physical stability of the system completely failed giving a "lost atoms" error. The problems with the stability of the system were solved by reducing the time step and reducing the strain rate. A suitable compromise was sought between the larger computational costs required for low time steps and the instability associated with larger time steps. The tests were performed at three different temperatures; 300K, 325K, 350K and kept at constant temperature during the process. The system was then analysed to determine the stress present in the model.

3. Results and Discussion

As opposed to the stress-strain diagrams derived from the conventional tensile testing, which presents a smooth curve with a linear slope in the elastic region; the stress-strain plot of the MD simulation is characterized by a series of steps of rise and fall. This behaviour can be attributed to strain hardening and subsequent softening of the material due to dislocation build up and rapid motion of the dislocations that follows [34]. A plot of the stress-strain curves for the composites at various temperatures are presented in Figure 2 (a-c). It can be observed that there is no clear distinction between the linear elastic range, the plastic range or the yield point. This lack of clear delineation creates difficulties in obtaining the values of the elastic moduli with appreciable degree of certainty. In this case, the modulus was obtained by fitting a second-degree polynomial to portions of the stress–strain diagram. All three graphs display similar trends. It is observed that the presence of the clusters of SiO_2 increased the yield strength of the base material (pure Al) which is subsequently reduced with the addition of more SiO_2. Further increasing the percentage of SiO_2 in the Al matrix uniformly reduces the ductility of the model.

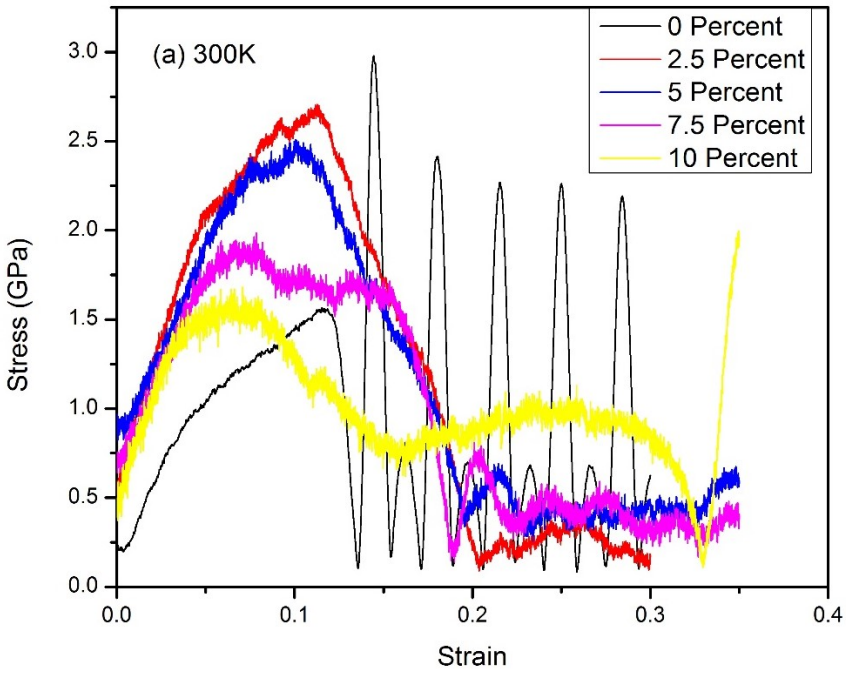

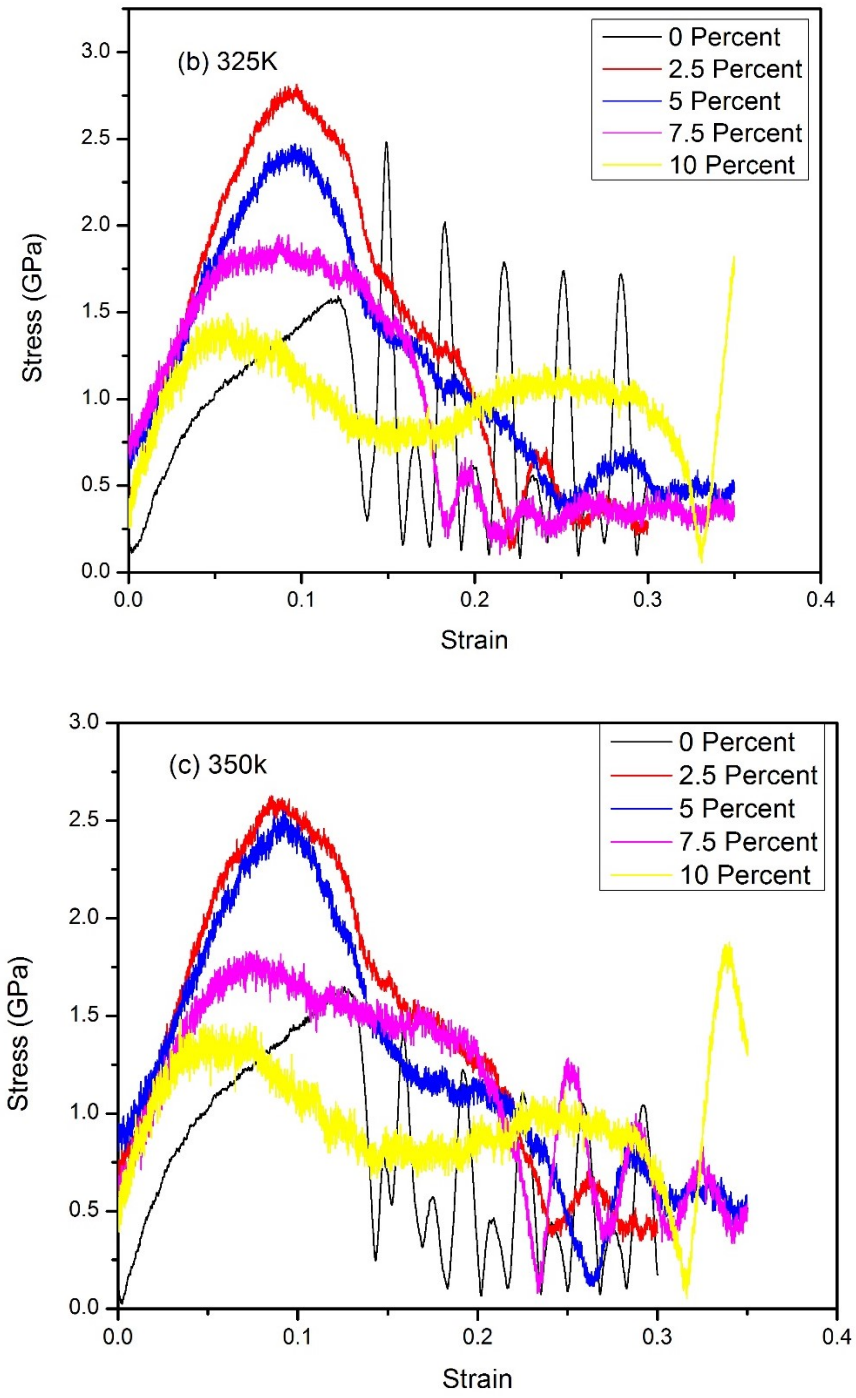

Figure 2: Tensile stress – Strain Plots at a) 300K. b) 325K. c) 350K

As shown in Figure 2(a-c), the clusters of SiO_2 disrupt the lattice of the pure Al and result in stress concentrations at the sites of infusion. As a result, an increase in the volume of SiO_2 used as reinforcement and an increase in temperature tends to reduce the tensile strength of the composites. To further understand this phenomenon, the Centrosymmetry tool in the OVITO software was used to visualise the change in the crystal structure of the composite by the addition of the SiO_2 clusters. The rendering of the OVITO analysis is presented in *Figure 3*. Clearly, the effects of the reinforcing phase on the crystallography of the base material can be observed. For instance, the sample containing 0wt%

SiO_2 had as high as 95% of the particles positioned in the standard FCC orientation which is expected of pure Aluminium. The sample with 2.5wt% SiO_2 had about 77.3% in the FCC configuration, the sample containing 5wt% SiO_2 had 62%, the sample containing 7.5wt %SiO_2 had 47.7% while the sample containing 10wt% SiO_2 had as low as 24.8% of the particles positioned in the FCC orientation. Quite clearly, with every increase in the percentage of SiO_2 in the composite, the crystal arrangement of the Al atoms was further disturbed. These disruptions occurred far beyond the local area/sites of infusion of SiO_2. However, because of the scale of samples studied using molecular dynamics, it is quite possible that the effective disruption to the crystallography of the base material on a much larger scale might be relatively less substantial than what was observed in this study. Animation of the tensile tests using OVITO showed that the atoms were substantially reorganized followed by rapid movement likely due to the generation of dislocations.

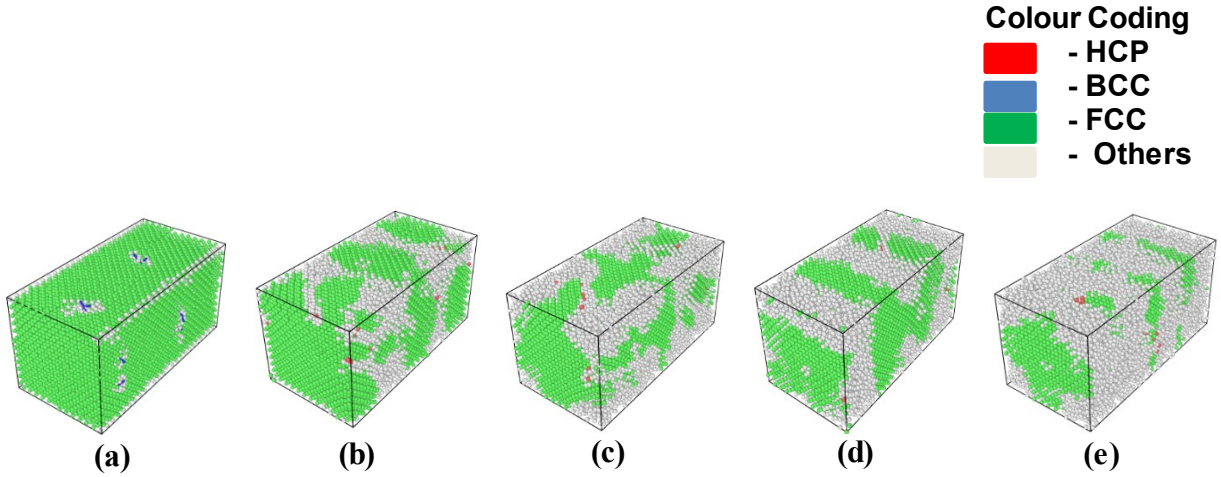

Figure 3: Distribution of Crystal Structures in composites at various wt% SiO_2; (a) 0wt% (b) 2.5wt%, (c) 5wt%, (d) 7.5wt%, (e) 10wt%

A snapshot of the process at different engineering strain values is displayed below in Figure 4 (a-e) for the different samples at 325K. Observation of the OVITO snapshots at similar strain values reveals that the pure aluminium (0 wt% SiO_2) fractures at lower strain value than the others. Furthermore, increasing the volume of SiO_2 in the composite results in lower strain values (i.e, increased brittleness) before the process of separation/fracture is observed.

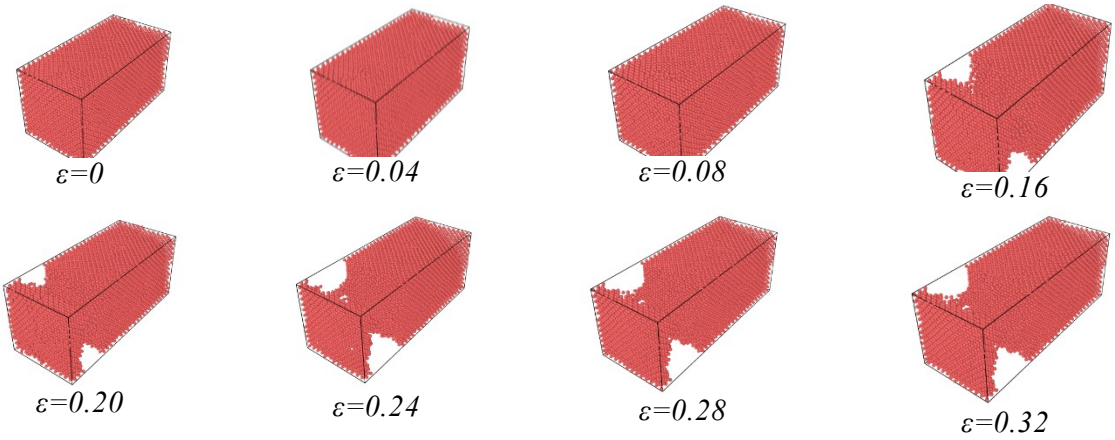

Figure 4a: Snapshots of the animation of the tensile tests with 0wt% SiO_2 at different strain values.

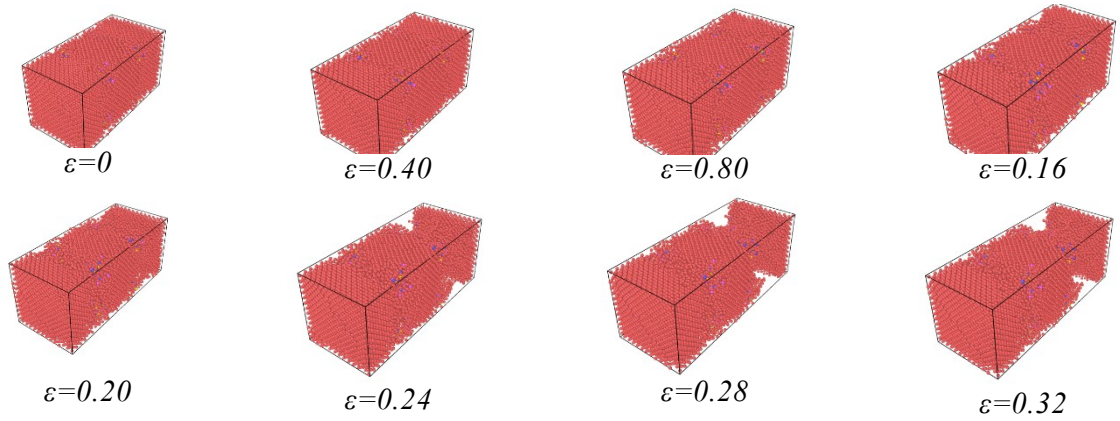

Figure 4b: Snapshots of the animation of the tensile tests with 2.5wt% SiO_2 at different strain values.

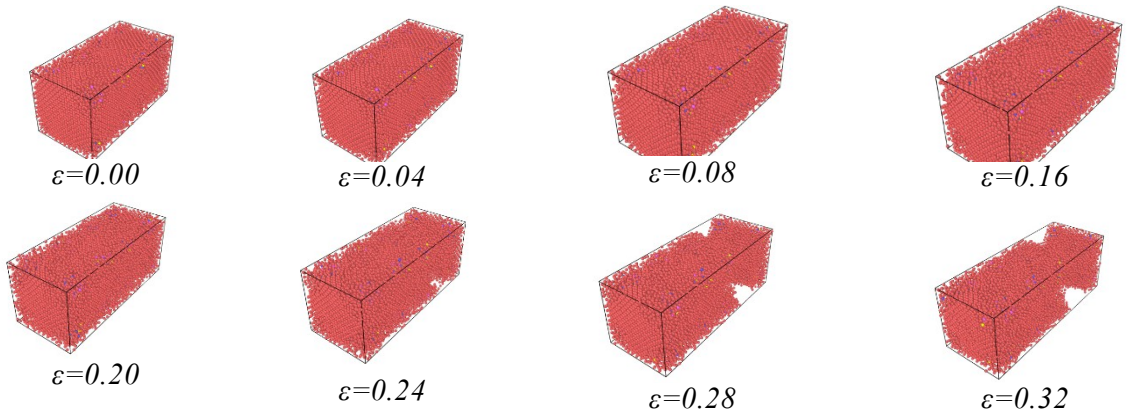

Figure 4c: Snapshots of the animation of the tensile tests with 5wt % SiO_2 at different strain values.

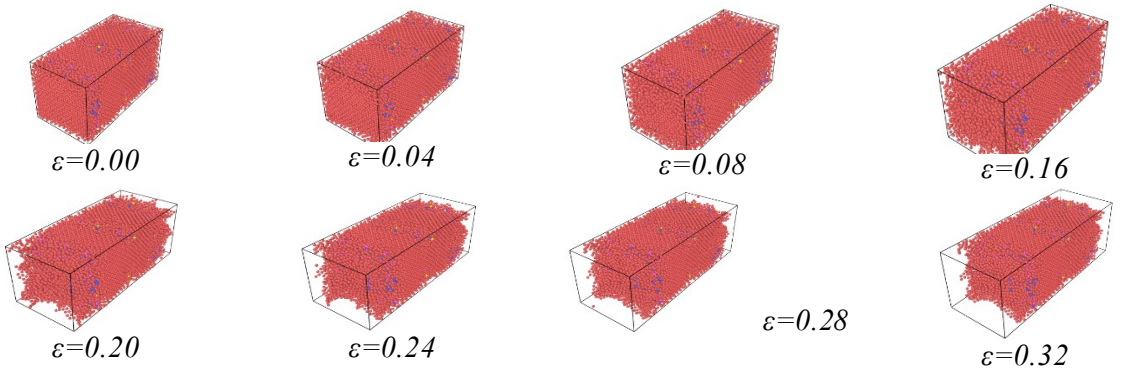

Figure 4d: Snapshots of the animation of the tensile tests with 7.5wt % SiO_2 at different strain values.

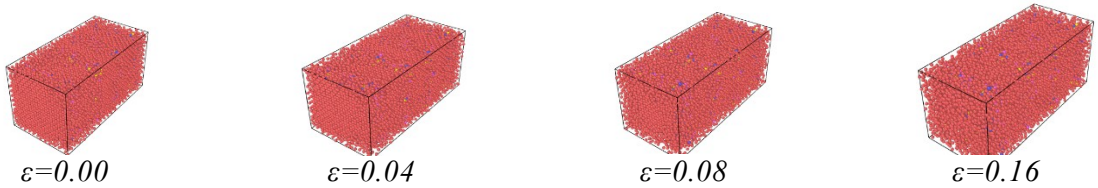

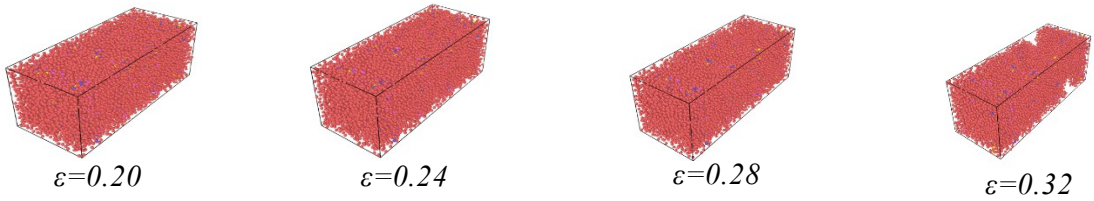

Figure 4e: Snapshots of the animation of the tensile tests with 10wt% SiO_2 *at different strain values.*

As mentioned earlier, there is substantial agglomeration around regions of SiO_2 with the reinforcing particles causing significant disruption to the otherwise perfect lattice of Al. As the sample is further stressed, the stress concentrations on those sites result in local stresses much higher than the average stress of the body, resulting in the initiation of cracks, propagation of the cracks and eventually resulting in the fracture/separation of the sample. The entire process can be easily monitored using the various tools available in OVITO. Figure 5 shows the Maximum stress distribution obtained at different temperatures. The results show that the maximum stress obtained for the composites decreased as temperature and wt% of SiO_2 increased. A maximum stress of 2.8141 GPa was obtained at 2.5wt% SiO_2 and a temperature of 325K. The lowest value of stress was 1.4946 GPa obtained at 325K and 10wt% SiO_2 reinforcement. At a temperature of 300K, the percentage change in stress were 73%, 60%, 27% and 7% at 2.5wt%SiO_2, 5wt%SiO_2, 7.5wt%SiO_2 and 10 wt%SiO_2 respectively.

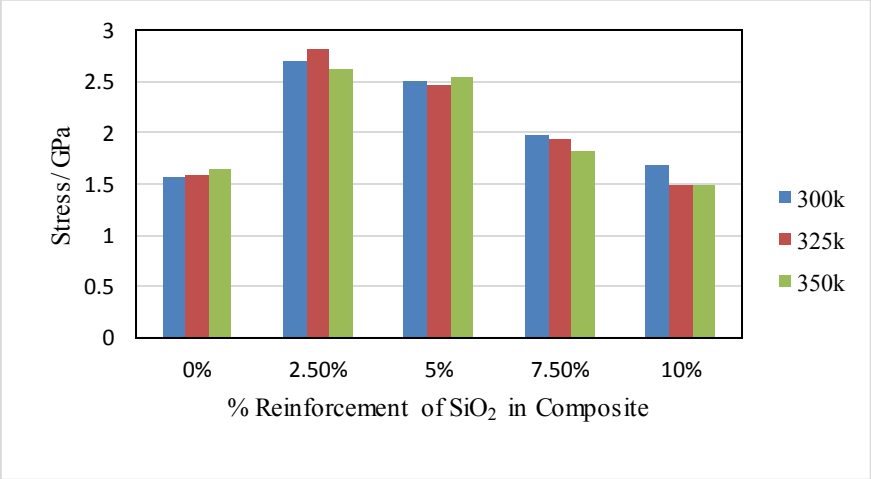

Figure 5: Maximum stress at 300K, 325K and 350K

From Figure 6, the Elastic modulus was observed to increase with increase in temperature, but decreased slightly with an increase in wt% of SiO_2. At 300K, 325k and 350k the Maximum elastic modulus of 25.30 GPa, 28.95 GPa and 43.23 GPa were obtained at 7.5wt% SiO_2, 2.5wt% SiO_2 and 10wt% SiO_2 respectively.

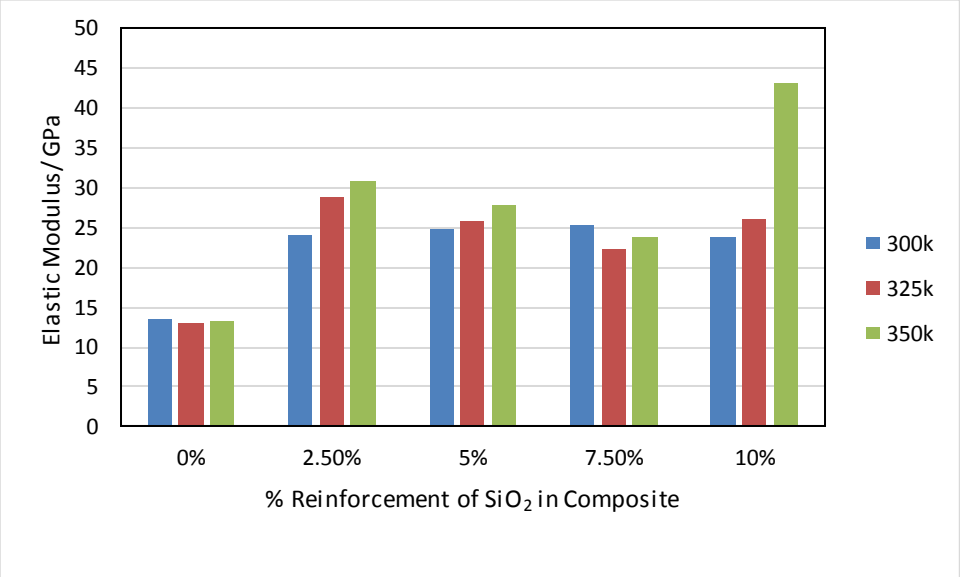

Figure 6: Elastic modulus at 300K, 325K and 350K

4. Conclusions

In this work, the elastic response of an Al- SiO_2 composite was studied. Molecular dynamics was used to characterise the behaviour of the composite. The results generally indicate that SiO_2 is suitable as a reinforcement for Al, and can result in substantial improvement in the mechanical properties of the base metal. A Maximum Elastic modulus of 43.3GPa was obtained at temperature of 350K and 10wt% SiO_2. The presence of the SiO_2 was found to substantially disrupt the FCC crystallography of the Al and reduce the ductility of the Al while substantially increasing the yield strength of the composite.

References

[1] R. Malik, S. Bhandari, A. Pant, A. Saxena, N. Kumar, N. Chotrani, D. Gunwant, P.L. Sah, Fabrication and Mechanical Testing of Egg Shell Particles Reinforced Al-Si Composites, Int. J. Math. Eng. Manag. Sci. 2 (2017) 53–62.

[2] S. Banerjee, B. V. Sankar, Mechanical properties of hybrid composites using finite element method based micromechanics, Compos. Part B Eng. 58 (2014) 318–327. doi:10.1016/j.compositesb.2013.10.065.

[3] Mruthyunjagouda, G. Manavendra, Experimental Investigation of Thermal behaviour on Rice Husk Ash-Alumina Reinforced with Al6063 Alloy Matrix, Int. J. Innov. Res. Sci. Eng. Technol. 6 (2017) 5454–5460. doi:10.15680/IJIRSET.2017.0604049.

[4] S.B. Hassan, V.S. Aigbodion, Effects of eggshell on the microstructures and properties of Al – Cu – Mg / eggshell particulate composites, J. King Saud Univ. - Eng. Sci. 27 (2015) 49–56. doi:10.1016/j.jksues.2013.03.001.

[5] J.A.K. Gladston, N.M. Sheriff, I. Dinaharan, J.D.R. Selvam, Production and characterization of rich husk ash particulate reinforced AA6061 aluminum alloy composites by compocasting, Trans. Nonferrous Met. Soc. China. 25 (2015) 683–691. doi:10.1016/S1003-6326(15)63653-6.

[6] S.S. Mukadam, A Review on Mechanical Behavior of Aluminium Metal with Different Reinforcing Materials, (2017) 3–6.

[7] R. Umunakwe, D.J. Olaleye, A. Oyetunji, O.C. Okoye, I.J. Umunakwe, Assessment of some Mechanical Properties and Microstructure of Particulate Periwinkle Shell-Aluminum 6063 Metal Matrix Composite (PPS-ALMMC) Produced by Two-Step Casting, Niger. J. Technol. 36 (2017) 421–427. doi:10.4314/njt.v36i2.14.

[8] K. Sinulingga, M. Sirait, A.M. Siregar, Addition of Nano Particles Effect of Rice Husk Ash as a Mixture On The Bricks Strength, IOP Conf. Ser. J. Phys. Conf. Ser. 1120 (2018) 1–9.

doi:10.1088/1742-6596/1120/1/012090.
[9] K. Kanayo, P. Apata, Original article Corrosion and wear behaviour of rice husk ash — Alumina reinforced Al – Mg – Si alloy matrix hybrid composites, J. Mater. Res. Technol. 2 (2013) 188–194. doi:10.1016/j.jmrt.2013.02.005.
[10] K.K. Alaneme, M.O. Bodunrin, A.A. Awe, Microstructure, mechanical and fracture properties of groundnut shell ash and silicon carbide dispersion strengthened aluminium matrix composites, J. King Saud Univ. - Eng. Sci. (2016). doi:10.1016/j.jksues.2016.01.001.
[11] K.K. Alaneme, O.J. Ajayi, Microstructure and mechanical behavior of stir-cast Zn–27Al based composites reinforced with rice husk ash, silicon carbide, and graphite, J. King Saud Univ. - Eng. Sci. (2015) 6–11. doi:10.1016/j.jksues.2015.06.004.
[12] H. Gu, X.-L. Gao, X.C. Li, Molecular Dynamics Study on Mechanical Properties and Interfacial Morphology of an Aluminum Matrix Nanocomposite Reinforced by -Silicon Carbide Nanoparticles, J. Comput. Theor. Nanosci. 6 (2009) 61–72. doi:https://doi.org/10.1166/jctn.2009.1007.
[13] S. Li, R.J. Arsenault, P. Jena, Quantum chemical study of adhesion at the SiC/Al interface, J. Appl. Phys. 64 (1988) 6246–6253. doi:10.1063/1.342082.
[14] B.K. Rao, P. Jena, Molecular view of the interfacial adhesion in aluminum-silicon carbide metal-matrix composites, Appl. Phys. Lett. 57 (1990) 2308–2310. doi:10.1063/1.103878.
[15] W. Lu, K. Zhang, X. Xie, Adsorption of a monolayer of iron on β-SiC(100) surfaces, Phys. Rev. B. 48 (1993) 18159–18163. doi:10.1103/PhysRevB.48.18159.
[16] S. Sharma, S.K. Tiwari, S. Shakya, Mechanical properties and thermal conductivity of pristine and functionalized carbon nanotube reinforced metallic glass composites: A molecular dynamics approach, Def. Technol. (2020). doi:https://doi.org/10.1016/j.dt.2020.04.004.
[17] H. He, Y. Rong, L. Zhang, Molecular dynamics studies on the sintering and mechanical behaviors of graphene nanoplatelet reinforced aluminum matrix composites, Model. Simul. Mater. Sci. Eng. 27 (2019) 18. doi:10.1088/1361-651X/ab2095.
[18] A. Stukowski, Visualization and analysis of atomistic simulation data with OVITO – the Open Visualization Tool, Model. Simul. Mater. Sci. Eng. 18 (2010) 1–8. doi:10.1088/0965-0393/18/1/015012.
[19] J.E. Lennard-Jones, On the determination of molecular fields.—I. From the variation of the viscosity of a gas with temperature, Proc. R. Soc. London. 106 (1924) 441–462. doi:https://doi.org/10.1098/rspa.1924.0081.
[20] J.E. Lennard-Jones, On the Determination of Molecular Fields. — II. From the Equation of State of a Gas., Proc. R. Soc. London A. 106 (1924) 463–477. doi:https://doi.org/10.1098/rspa.1924.0082.
[21] M.S. Daw, M.I. Baskes, Embedded-atom method: Derivation and application to impurities, surfaces, and other defects in metals, Phys. Rev. B. 29 (1984) 6443–6453. doi:10.1103/PhysRevB.29.6443.
[22] M. Baskes, Modified embedded atom method calculations of interfaces., Sandia. 96 (1996).
[23] J.E. Angelo, M.I. Baskes, Interfacial Studies Using the EAM and MEAM, Interface Sci. 63 (1996) 47–63.
[24] K. Gall, M.F. Horstemeyer, M. Van Schilfgaarde, M.I. Baskes, Atomistic simulations on the tensile debonding of an aluminum – silicon interface, J. Mech. Phys. Solids. 48 (2000) 2183–2212.
[25] D.K. Ward, W.A. Curtin, Y. Qi, Mechanical behavior of aluminum – silicon nanocomposites : A molecular dynamics study, Acta Mater. 54 (2006) 4441–4451. doi:10.1016/j.actamat.2006.05.022.
[26] J.-K. Kim, S.C. Tjong, Y.-W. Mai, Effect of Interface Strength on Metal Matrix Composites Properties, Elsevier Ltd., 2018. doi:10.1016/B978-0-12-803581-8.09982-3.
[27] N. Yedla, R. Nalla, S. Pal, P. Gupta, M. Meraj, Molecular Dynamics Studies on the Prediction of Interface Strength of Cu(metal)-CuZr (metallic glass) Metal Matrix Composites, (n.d.).
[28] P. Gupta, N. Yedla, High Temperature Mechanical Behavior of Aluminum- Cu50Zr50 Metallic Glass Interface, IOP Conf. Ser. Mater. Sci. Eng. 115 (2016). doi:10.1088/1757-

899X/115/1/012024.
[29] S. Schmauder, S. Hocker, P. Kumar, Molecular dynamics simulations of tensile tests and interfacial fracture in, ResearchGate. (2010) 1–9.
[30] P. Sedigh, A. Zare, A. Montazeri, Evolution in aluminum applications by numerically-designed high strength boron-nitride / Al nanocomposites, Comput. Mater. Sci. 171 (2020) 109227. doi:10.1016/j.commatsci.2019.109227.
[31] M.E. Suk, Enhanced tensile properties of weight-reduced nanoporous carbon nanotube-aluminum composites, Mater. Express. 9 (2019) 801–807. doi:10.1166/mex.2019.1561.
[32] C.R. Dandekar, Y.C. Shin, Effect of porosity on the interface behavior of an Al 2 O 3 – aluminum composite : A molecular dynamics study, Compos. Sci. Technol. 71 (2011) 350–356. doi:10.1016/j.compscitech.2010.11.029.
[33] C.R. Dandekar, Y.C. Shin, Effect of porosity on the interface behavior of an Al 2 O 3 – aluminum composite : A molecular dynamics study, Compos. Sci. Technol. 71 (2011) 350–356. doi:10.1016/j.compscitech.2010.11.029.
[34] R. Komanduri, N. Chandrasekaran, L.M. Raff, Molecular dynamics (MD) simulation of uniaxial tension of some single-crystal cubic metals at nanolevel, Int. J. Mech. Sci. 43 (2001) 2237–2260.